Role of lipophilicity on the activity of hexameric cyclic peptoid ion carriers

R. Schettini,[a] Massimo Tosolini,[b] Jawad ur Rehman,[b],[c] Muhammad Raza Shah,[c] G. Pierri,[a] C. Tedesco,[a] G. Della Sala,[a] F. De Riccardis,[a] Paolo Tecilla,*[d] and I. Izzo*[a]

[a] Dott. R.Schettini, Dott. G. Pierri, Prof. C. Tedesco, Prof. G.Della Sala, Prof. F. De Riccardis, Prof. I. Izzo
Dipartimento di Chimica e Biologia "A. Zambelli"
Università degli Studi di Salerno
Via Giovanni Paolo II, 132, 84084 Fisciano, Salerno, (Italy).
E-mail: iizzo@unisa.it

[b] Dott. M Tosolini, Dott. J. ur Rehman,
Dipartimento di Scienze Chimiche e Farmaceutiche,
Università degli Studi di Trieste,
Via Giorgieri 1, 34127 Trieste (Italy).

[c] Dott. J. ur Rehman, Prof. M. Raza Shah
H.E. J. Research Institute of Chemistry, International Center for Chemical and Biological Sciences
University of Karachi
Karachi-75270 Pakistan.

[d] Prof. P. Tecilla
Dipartimento di Matematica e Geoscienze
Università degli Studi di Trieste
Via Weiss 8, 34127 Trieste (Italy),
E-mail: ptecilla@units.it
https://www.units.it/persone/index.php/from/abook/persona/5958

Supporting information for this article is given via a link at the end of the document.((Please delete this text if not appropriate))

Abstract: Two families of hexameric cyclic peptoids decorated with linear *N*-alkyl and alternated *N*-alkyl/*N*-benzyl side chains (**2a-d** and **3a-c**, respectively) were designed and synthesized in order to correlate their logP values (from 2.55 to 6.83) to their ionophoric activities. The present contribution confirms the general ability of hexameric cyclic peptoids to behave as efficient cation carriers, corroborates their preference for Na^+ ion, among the tested alkali metals, and suggests a Na^+/H^+ antiport transport mechanism (rate limited by the transport of the proton) for these new ionophores. Our observations indicate that in order to attain an efficient ionophoric activity, a narrow range of liphophilicity is required (4< logP < 5). Moreover, to gain information on the solid state stucture of ionophoric cyclic peptoids with linear *N*-side chains, X-ray crystallographic studies were performed on exemplar compound **2a**. Crystal structure of compound **2a** confirms the tendency of ionophoric cyclopeptoids with linear *N*-side chains to form layered assemblies.

Introduction

Cyclic peptoids (cyclic *N*-substituted oligoglycines) are known to efficiently and selectively transport cations across phospholipid membranes for their close structural resemblance to natural cyclic depsipeptide ionophores (such as valinomycin[1] and enniatins).[2]

Their functional properties were first demonstrated for landmark cyclic peptoid **1** (Figure 1),[3] acting as mobile carrier and showing a preference for Na^+ ion (compared to other alkaline cations). In the mobile carrier mechanism,[4] the ion transporter resides in the membrane and binds the charged species at the interface between the lipid and aqueous phase. In the non-electrogenic antiport mechanism the carrier-ion complex moves freely inside the nonpolar phase promoting an ion flux across the membrane in favour of the concentration gradient counterbalanced by the back-transport of a different ion of the same charge (Figure 1).

Two main factors can affect the transport process: the ion affinity and the lipophilicity of the carrier. As expected in structurally related classes of compounds, generally, the best receptors are the most effective carriers,[5] although a too strong affinity may slow down the transport process.[6] On the other hand, several studies have demonstrated that there is an optimal value for the lipophilicity of the carrier and that too hydrophilic or too lipophilic carriers usually display low transport activity.[7] This translates in a bell shaped dependence of the transport activity from the lipophilicity of the carrier, frequently described using the octanol/water partition coefficient (logP), with the position of the maximum depending from the structure of the carrier.[7a] A compromise between the need of the carrier to reach the water/membrane interphase, where the ion complexation process takes place, and to form a membrane soluble complex ought to be obtained. In this scheme, highly hydrophilic carriers do not diffuse trough the membrane while too lipophilic carriers are buried in the membrane and do not reach the interphase with water. Moreover, highly nonpolar carriers may fail to reach the membrane because they precipitate out from the water solution when added to preformed liposomes.[8] Interestingly, while this behaviour

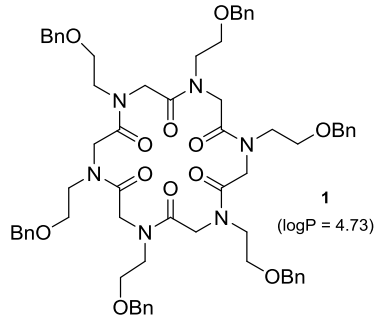

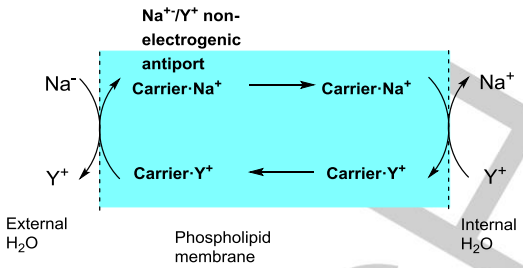

has been well described in the case of anion transport,[9] it has been less investigated in the transport of cations.[10]

Figure 1. Structure of cyclic peptoid **1** and schematic representation of the mobile carrier non-electrogenic cation transport mechanism.

Previous studies on ion transport properties of cyclic peptoids suggest that both affinity[11] for the transported cations and lipophilicity[12,13] of the carrier influenced their activities with good ion transport activities clustering in a logP range between 4 and 5. However, the obtained data emerged from structurally non-homogeneous series of compounds and it is known that the substitution pattern has a significant impact on these type of correlations.[7a] We, therefore, decided to prepare two relatively homogeneous families of hexameric cyclic peptoids bearing linear C_3, C_5-C_7 *N*-alkyl substituents plus alternating linear C_3, C_4, C_5 *N*-alkyl/*N*-benzyl substituents (**2** and **3** in Figure 2). The hexameric motif was conserved in all compounds to have the same ion recognition ability while the side chains were chosen in order to test an ample range of lipophilicity. The presence of the benzyl group obviated crucial solubility problems experienced with some full linear cyclohexameric counterparts.

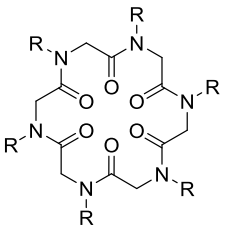

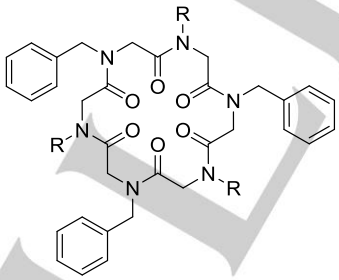

2a: R = -$(CH_2)_2CH_3$, logP = 2.55
2b: R = -$(CH_2)_4CH_3$, logP = 5.04
2c: R = -$(CH_2)_5CH_3$, logP = 5.96
2d: R = -$(CH_2)_6CH_3$, logP = 6.83

3a: R = -$(CH_2)_2CH_3$, logP = 3.61
3b: R = -$(CH_2)_3CH_3$, logP = 4.40
3c: R = -$(CH_2)_4CH_3$, logP = 5.18

Figure 2. Structure of the new cyclic peptoids **2a-d** and **3a-c**. The logP values of reported compounds were calculated using the ALOGPs 2.1 software.

Here we report the synthesis and the characterization of new cyclic peptoids **2a**, **2d** and **3a-c**. The study of their ionophoric activity indicates that also within this class of cation transporters the lipophilicity of the carrier is a highly relevant parameter and that a narrow range of lipophilicity is required (4< logP < 5) to ensure high cation transport rates.

Results and Discussion

Synthesis

Target compounds **2a-d**[14] and **3a-c** were obtained from the corresponding linear oligomers elongated on the 2-chlorotrityl solid support using the "submonomer" approach.[15] This method consists in a series of iterated acylation reactions with bromoacetic acid (mediated by *N,N*-diisopropylcarbodiimide, DIC), and S_N2 substitutions (with the proper primary amine). When ready, the requested linear peptoids were cleaved from the resin using the slightly acidic 1,1,1,3,3,3- hexafluoro-2-propanol (HFIP) and cyclized under high dilution conditions (3.0×10^{-3} M) in the presence of HATU.[16] Precipitation from hot ethyl acetate afforded cyclohexamers **2a-d** and **3a-c** in acceptable yields (Figure 2, 34-50%). Their room temperature ^{1}H-NMR spectra revealed the presence of multiple conformers in slow equilibrium on the NMR time scale.[17]

Stepwise quantitative addition of NaTFPB indicated formation of "rigid" symmetric metalated species (as evident for **3a**, Figure 3).

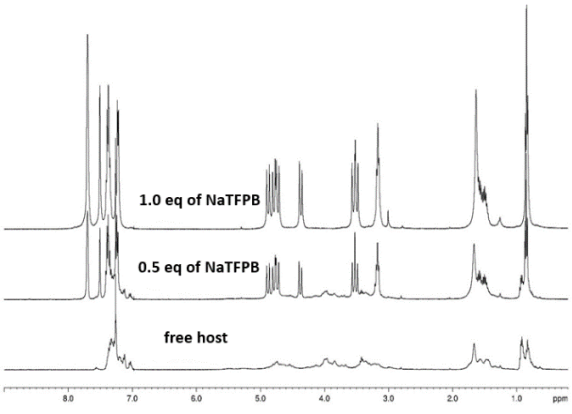

Figure 3. ^{1}H NMR spectra reporting the quantitative stepwise addition of NaTFPB to **3a** (400 MHz, $CDCl_3$, 298 K, 10.0 mM solution).

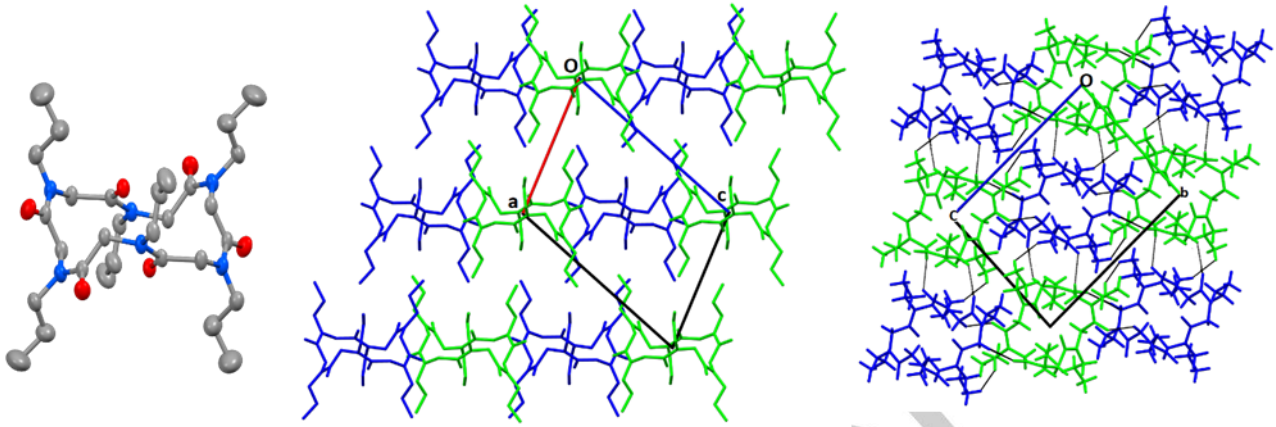

Figure 4. Left: X-ray molecular structure of **2a** type II molecule. For clarity, ellipsoids are drawn at 30% probability level and hydrogen atoms are omitted. Middle: Crystal packing of **2a** as viewed along the *b* axis to highlight the layered assembly. Type I molecule in blue, type II molecule in green. For clarity, hydrogen atoms are omitted and only one possible site is displayed for the disordered atoms. Right: CO··· CH intralayer interactions involving backbone carbonyl oxygen atoms of type I molecules and methylene hydrogen atoms of type II molecules, and vice versa.

X-ray crystallography

Crystals of compound **2a**, suitable for X-ray diffraction analysis, were obtained by slow evaporation from a hot ethyl acetate solution. The obtained crystals showed a triclinic unit cell with two crystallographically independent cyclopeptoid molecules in the asymmetric unit. Type I and type II molecules are depicted in blue and green, respectively, in Figure 4, they differ only slightly in the side chains positions. In particular, in type I molecule the *cis* side chains attached to the N1A nitrogen atom are disordered. Both type I and type II molecules are located on a crystallographic inversion centre and display a distorted *cctcct* peptoid backbone conformation (where *c* denotes *cis* and *t trans* tertiary amide junctions) with side chains pointing alternatively up and down with respect to the macrocycle plane (Figure 4, left). As previously reported by us,[14b] the vertical positioning of the side chain seems to be a distinct feature of cyclopeptoids decorated with linear *N*-alkyl side chains.

The crystal packing of compound **2a** displays a layered assembly of peptoid macrocycles resembling to a lipid bilayer (Figure 4, middle). The solid state interactions can be divided into intralayer and interlayer interactions. Intralayer interactions consist mainly of CH···OC backbone to backbone interactions, involving backbone carbonyl oxygen atoms of type I molecules and methylene hydrogen atoms of type II molecules, and vice versa (Figure 4, right). Interlayer interactions involve the vertical *N*-alkyl side chains.

Ionophoric activities

The ability of the new cyclic peptoids to transport Na^+ across a liposomal phospholipid membrane was assessed using the standard HPTS assay (Figure 5).[18] In this experiment HPTS (8-hydroxypyrene-1,3,6-trisulfonic acid), a water soluble fluorescent pH indicator with a pKa of 7.2, is trapped in the inner water pool of large unilamellar vesicles (LUVs, 100 nm diameter) made by egg yolk phosphatidylcholine (EYPC). The lipid suspension is prepared in water buffered at pH 7 and containing 100 mM NaCl. Then a pH gradient is established across the phospholipid membrane by external addition of NaOH. The increase of the HPTS fluorescence emission in response to the applied transmembrane pH-gradient indicates basification of the inner water pool which may be derived either from H^+ efflux or OH^- influx. This transmembrane charge translocation needs to be counterbalanced by a concurrent movement of other ions. In the case of hexameric cyclic peptoids, it has been shown that they promote a H^+/Na^+ antiport in which the transport of H^+ from inside to outside the liposome is balanced by the opposite transport of a sodium ion (Figure 5).[12,13] As a consequence, the increase in HPTS emission is directly related to the transport of Na^+ across the phospholipid membrane. In addition, the standard HPTS assay can be easily modified to investigate the cation or anion selectivity in the transport process.[19] In this case, the liposomes are prepared in HEPES buffer containing NaCl 100 mM and diluted with the same buffer but containing 100 mM of MCl (M = Li^+, Na^+, K^+, Rb^+, Cs^+) or NaX (X = Cl^-, Br^-, I^-). The base pulse is given using the appropriate MOH solution and the pH gradient can be discharged by different mechanisms which, limiting the discussion to ions antiport, are H^+/M^+ or OH^-/Cl^- exchange in cation selectivity experiments and H^+/Na^+ or

OH^-/X^- exchange in anion selectivity experiments (Figure 5, bottom). Independence of the transport rates from the anion or cation present indicates preference for cation or anion transport, respectively, while the measurements of the transport rates in the presence of the different ions allows to determine the ion selectivity of the carrier.

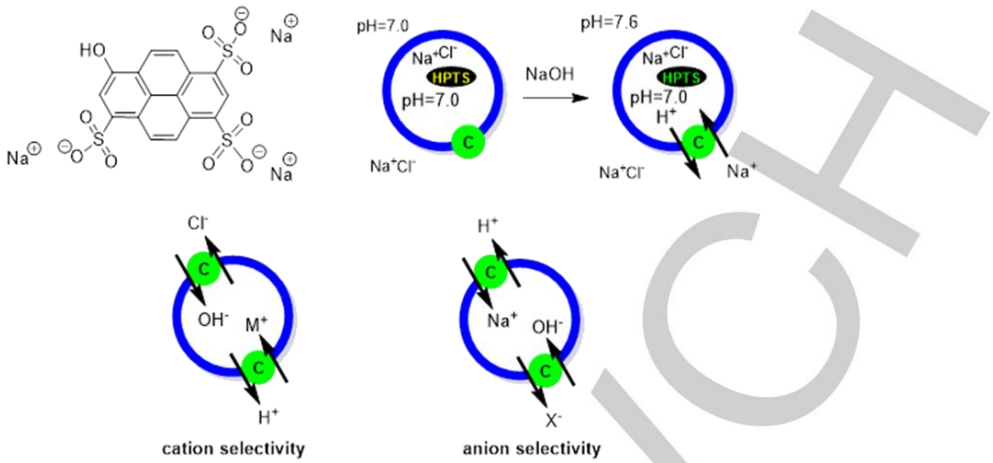

Figure 5. Top: structure of HPTS (left) and schematic illustration of the HPTS assay (right) in which a carrier (C, green circle) promotes the antiport of H^+ and Na^+. Bottom: possible ion antiport processes in HPTS ion selectivity assays.

Figure 6a and 6b report the kinetic profiles recorded in the HPTS assay using cyclopeptoids **2a**-**d** and Na^+ as transportable cation in the absence and in the presence of the protonophore CCCP (carbonyl cyanide 3-chlorophenylhydrazone), respectively. In the case of compounds **2a**-**c** the ionophore was added to the preformed liposomes before to start the kinetic experiment (single side addition) while for the more lipophilic **2d** it was necessary to pre-incorporate the peptoid during the swelling of the lipids before preparation of the liposomes (double side addition). Indeed, single side addition with **2d** failed to reveal any ionophoric activity probably because the compound precipitated out of the water solution and was not able to partition into the liposomes. The results of Figure 6a,b show that all the cyclic peptoids are able to transport Na^+ across the phospholipid membrane, although with different activities, and that addition of CCCP has a general accelerating effect on the transport kinetics. This latter effect has been observed with other cyclic peptoids[12,13] and it is related to an H^+/Na^+ antiport mechanism in which the proton transport is rate limiting. CCCP is an electrogenic proton carrier and it is able to promote a unidirectional and not counterbalanced proton flux, thus decoupling the H^+ and Na^+ transport processes. Therefore, the data obtained with CCCP reflected the intrinsic ability of the carrier to transport the metal cation not influenced by its ability to back-transport the proton. As expected for hexameric cyclic peptoids[3Errore. Il segnalibro non è definito.] they transport selectivity Na^+ while the other alkaline metal cations are practically not transported. This is shown in Figure 6c for compounds **2c** while the results obtained with the other cyclic peptoids are shown in the ESI (Figure S23). As shown in Figures 6a and 6b in the absence of CCCP the most active compound is **2b** (logP = 5.04) while in the presence of CCCP **2c** (logP = 5.96) was found more active. However, when trying to investigate the dependence of the transport activity on the ionophore concentration, in particular for the most active **2b** and **2c**, we noted an unexpected low reproducibility of the kinetic data within different and even within the same preparation of liposomes. For instance, eight repetitions of the kinetic at 5% concentration of ionophore in the presence of 1% CCCP gave average rate constants of k_t = 0.007 ± 0.004 s^{-1} and k_t = 0.009 ± 0.003 s^{-1} for **2b** and **2c**, respectively. This high uncertainty in the determination of the rate constants did not allow to identify the most active carrier between the two cyclopeptoids and may likely also be the reason for the inversion of activity observed in Figure 6 in the absence and presence of CCCP. To face the problem, we tried to increase the incubation time of the ionophore in the liposome suspension before to start the kinetic and to pre-incorporate the peptoids in the phospholipid membrane but without appreciable improvements of the quality of the data. This unexpected, and never observed before for this class of compounds, low reproducibility of the kinetic experiments is probably a consequence of their low solubility in water which may favor the formation of small aggregates. This behavior may be correlated to the presence of only linear alkyl substituents on the cyclic peptoid ring. Indeed, the X-ray crystal structures of **2a** (Figure 4), **2b** and **2c**,[14b] show the formation in the solid state of layers of macrocycles where CO···HC interactions between carbonyl oxygen atoms and methylene hydrogen atoms belonging either to backbone or *N*-alkyl side chains contribute to stabilize a layered assembly in which the alkyl chains are in close contact.[14b] Although we do not have direct experimental evidences of the formation of such ordered structures in solution, the linear alkyl substitutes may favor an aggregation process due to their tendency to interdigitate and this process may be randomly influenced by factors like, for example, stirring rate and speed of the addition of the ionophore solution to the liposome suspension, thus influencing the actual concentration of the ionophore in the membrane and, eventually, its activity. For this reason, we designed and prepared cyclopeptoids **3** in which linear *N*-alkyl side chains alternate with *N*-benzyl substitutes. As a matter of fact, these compounds behaved much better

showing a good reproducibility of the kinetic experiments with standard deviations of the values of the rate constants in the order of 5%, as usually observed.

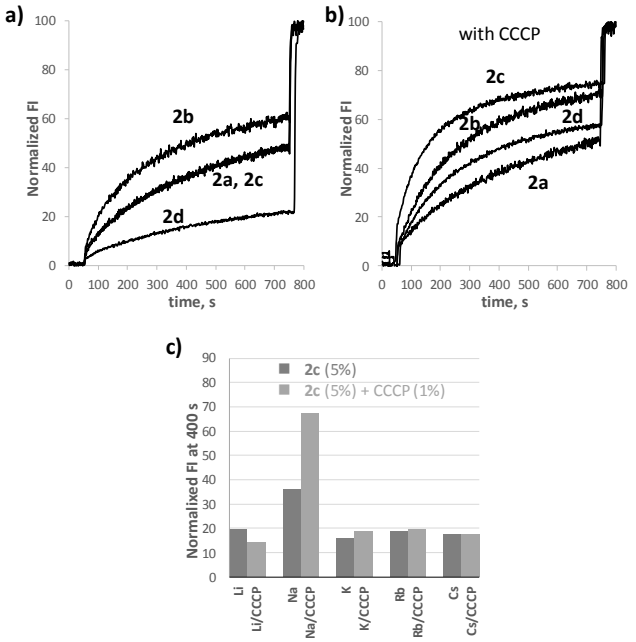

Figure 6. Normalized fluorescence change in HPTS fluorescence emission (FI) as a function of time after addition of the base (50 µL of 0.5 M NaOH) to EYPC LUVs (100 nm diameter) loaded with HPTS (0.1 mM HPTS, 0.17 mM total lipid concentration, 25 mM HEPES, 100 mM NaCl, pH 7.0, total volume: 3 mL), in the presence of cyclopeptoids **2a**–**2d** (5% concentration) in the absence (a) and in the presence (b) of CCCP (1% concentration). The concentrations are given in mol% with respect to the concentration of lipids; (c) cation selectivity for cyclopeptoid **2c** (5 mol%) in the absence and in the presence of CCCP (1%), using the HPTS assay (100 mM MCl, pH 7.0, base pulse by addition of 50 µL of 0.5 M MOH). The transport activity is reported as the normalized fluorescence intensity measured at 400 s.

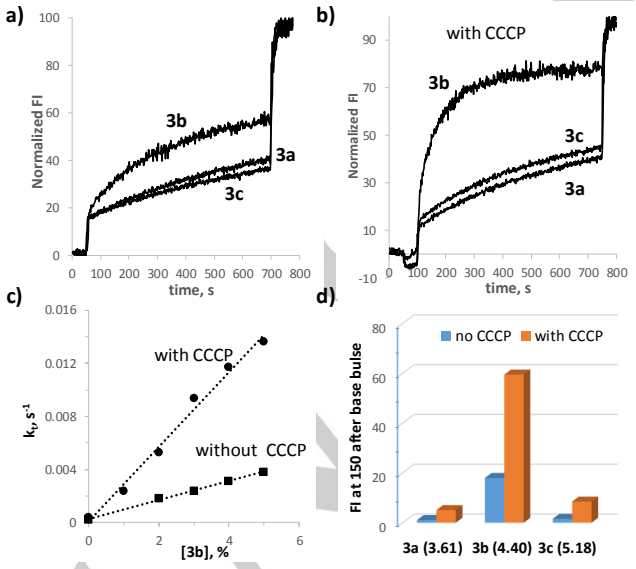

Figure 7. Normalized fluorescence change in HPTS fluorescence emission (FI) as a function of time after addition of the base (50 µL of 0.5 M NaOH) to EYPC LUVs (100 nm diameter) loaded with HPTS (0.1 mM HPTS, 0.17 mM total lipid concentration, 25 mM HEPES, 100 mM NaCl, pH 7.0, total volume: 3 mL), in the presence of cyclopeptoids **3a**-**3c** (5% concentration) in the absence (a) and in the presence (b) of CCCP (1% concentration). The concentrations are given in mol% with respect to the concentration of lipids; (c) dependence of the first order rate constant for the Na^+ transport process (k_t, s^{-1}) on the concentration of **3b** in the presence (●) and in the absence of CCCP (■). The Figure reports the first order rate constants obtained by the fitting of the kinetic profiles reported in Fig. S26; (d) normalized fluorescence intensity measured at 150 s after the base pulse and corrected for the FI of the blank experiment for cyclopeptoids **3a-c** at 5% concentration. In brackets are reported the calculated logP of the cyclopeptoids.

Figure 7a and 7b report the kinetics profiles recorded with the HPTS assay at a 5% concentration of cyclopeptoids **3** in the absence and in the presence of CCCP (1%), respectively. In the absence of CCCP only **3b** shows some activity while **3a** and **3c**, after an initial and instant jump of fluorescence intensity due to some HPTS not trapped inside the liposomes, show a very slow increase in fluorescence intensity almost superimposable with the control experiment recorded in the absence of ionophore (see ESI, Fig S24 and S25). Addition of CCCP strongly accelerates the transport kinetic of **3b** while the effect on the other two cyclic peptoids is much less pronounced. The low activity of **3a** and **3c** was confirmed with experiments at different concentrations of ionophores showing very little dependence of the Na^+ transport kinetics on the concentration of cyclic peptoids (ESI, Fig S24 and S25). On the contrary **3b** shows an evident concentration/activity dependence both in the absence and in the presence of CCCP as shown in Figure 7c which reports the Na^+ transport rate constants in function of the **3b** concentration and Figure S26, in the ESI, where are reported the original kinetic profiles. Figure 7d shows the normalized fluorescence intensity measured at 150 s after the base pulse in the presence of 5% **3a-c** and corrected for the FI of the blank experiment. In brackets are also reported the logP values of the cyclopeptoids which increase on going from **3a** to **3c**. Taking in account that the molecular structure of cyclopeptoids **3a-c** is the same, differing only for the lengths of the alkyl residues which influences only their lipophilicity, the maximum activity observed for **3b** whit a logP intermediate between **3a** and **3c** suggests that the transport process is very sensitive to the lipophilicity of the carrier and activity is observed in a very narrow window of logP values.

To better define the mechanism of transport of cyclopeptoid **3b** we investigated its cation and anion selectivity and the effect of addition of cholesterol to the phospholipid membrane on the rate of the transport process. Figure 8 reports the results obtained in the study of the anion and cation selectivity. Both in the absence and in the presence of CCCP **3b** transports Na^+ more efficiently that the other alkaline metal cations. On the other hand, keeping Na^+ as transportable cation and changing the counter anion from chloride, to bromide and to iodide the transport efficiency was not influenced by the different anions, suggesting that in all the cases the observed transport process is the transport of the Na^+ cation. Overall, this sensitivity of the transport process to the nature of the cation and insensitivity to the nature of the anion indicates that **3b** transport cations, preferentially Na^+, and not anions. As expected, experiments with Li^+, Na^+ and K^+ using **3a** and **3c** and CCCP did not show any relevant transport phenomena (See ESI Fig S27).

Figure 9 reports the first order rate constants for the Na^+ transport process promoted by **3b** in the absence and in the presence of CCCP and of cholesterol in the membrane (70 : 30

EYPC/cholesterol lipid composition). Both in the absence and in the presence of CCCP, cholesterol has a major slowing down effect on the transport process. This is consistent with a mobile carrier mechanism because cholesterol makes the membrane less fluid thus slowing down the rate of transport of carrier-like ionophores.[20] Overall, all these data indicate that **3b** selectively transports Na^+ with a mobile transport mechanism in which the antiport of the proton limits the rate.

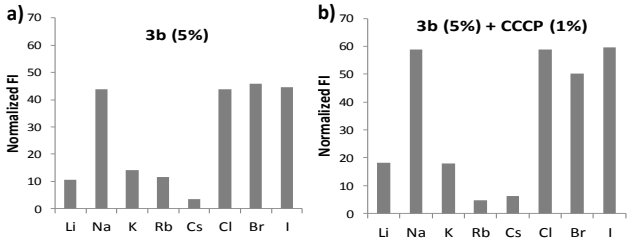

Figure 8. Cation and anion selectivity for cyclopeptoid **3b** (5 mol%) in the absence (a) and in the presence of 1% CCCP (b), using the HPTS assay (100 mM MCl, pH 7.0, base pulse by addition of 50 µL of 0.5 M MOH for cation selectivity and 100 mM NaX, pH 7.0, base pulse by addition of 50 µL of 0.5 M NaOH for anion selectivity). The transport activity is reported as normalized fluorescence intensity measured at 350 s and 150 s after the base pulse for the experiment in the absence and in the presence of CCCP, respectively, and corrected for the FI of the blank.

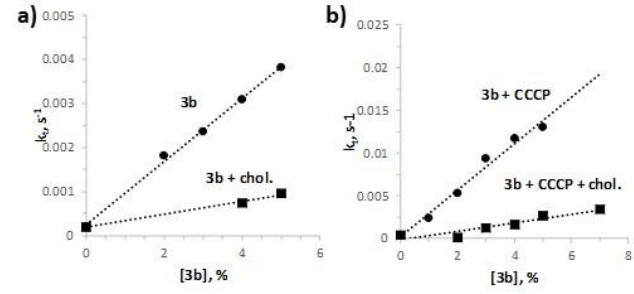

Figure 9. Dependence of the first order rate constant of the Na^+ transport process (k_t, s^{-1}) on the concentration of **3b** in liposome containing cholesterol (EYPC : Chol 70 : 30, ■) and without cholesterol (●) in the absence (a) and in the presence of 1% CCCP (b). The original kinetic profiles are reported in Fig. S28 in the ESI.

Conclusion

In the present work, we have conducted a systematic study in order to relate the lipophilicity of designed hexameric peptoids (with linear *N*-alkyl and alternated *N*-alkyl/*N*-benzyl side chains) to their Na^+ transport abilities. The results confirmed that hexameric cyclopeptoids are efficient M^+/H^+ antiport carriers (with a preference for Na^+ among the alkali metal ions). Our results suggest that lipophilicity (measured in term of logP parameter) is a very important factor influencing the transport ability of the carrier and that a logP value ~ 4.4 is optimal for ion translocation. The ample bouquet of peptoid analysed also showed the intrinsic limits of hexameric peptoids with all-linear *N*-side chains. Intermolecular interactions (highlighted by the X-ray crystal structure of **2a**, **2b** and **2c** cyclic peptoids)[14b] may favour formation of small aggregates that can impair the transport abilities of those cyclooligomers. However, presence of benzyl side chains replenishes the translocation properties of cyclic peptoids. In conclusion the results obtained for cyclopeptoid-based ion carriers, offer reliable guidelines for the design of new, more efficient, cyclooligomeric systems, and represent a contribution towards the understanding of their action in liposome systems. Our further step is to translate those background studies in novel bioactive leads with antibiotic activities.

Experimental Section

General procedure for synthesis of compounds 2 a-d and 3 a-c
General information. Starting materials and reagents purchased from commercial suppliers were generally used without purification unless otherwise mentioned. Reactions were monitored by analytical thin layer chromatography (TLC) on precoated silica gel plates (0.25 mm) and visualized by UV light. The purity grade of cyclic peptoids were checked by HPLC analysis using a C18 reversed-phase analytical column (Bondapak, 10 µm, 125 Å, 3.9 mm × 300 mm) run with linear gradients of ACN (0.1% TFA) into H_2O (0.1% TFA) over 30 min, at a flow rate of 1.0 mL/min, using a Modular HPLC System JASCOLC-NET II/ADC equipped with a JASCO Model PU-2089 PlusPump and a JASCO MD-2010 Plus UV-vis multiple wavelength detector set at 220 nm. High resolution mass spectra (HRMS) were recorded on a Bruker Solarix XR Fourier transform ion cyclotron resonance mass spectrometer (FTICR-MS) equipped with a 7T magnet, using matrix-assisted laser desorption/ionization (MALDI). Elemental analyses were performed with a Thermo FlashEA 1112 Series CHNS−O analyzer by Thermo Fisher ScientificInc. (Waltham, MA, USA); the samples were analyzed after extensive drying in vacuo. Yields refer to chromatographically and/or spectroscopically (^{1}H- and ^{13}C NMR) pure materials. ^{1}H NMR and ^{13}C spectra were recorded on Bruker DRX 600 (^{1}H at 600.13 MHz, ^{13}C at 150.90 MHz) and Bruker DRX 400 (^{1}H at 400.13 MHz, ^{13}C at 100.03 MHz). Chemical shifts (δ) are reported in ppm relative to the residual solvent peak ($CHCl_3$, δ = 7.26; $^{13}CDCl_3$, δ = 77.0) and the multiplicity of each signal is designated by the following abbreviations: s, singlet; d, doublet; t, triplet; m, multiplet; bs, broad singlet; bd, broad doublet. Coupling constants (*J*) are quoted in Hertz.

General procedure for the synthesis of linear peptoids
2-chlorotrityl chloride resin (2,α-dichlorobenzhydryl-polystyrene cross-linked with 1% DVB; 100–200 mesh; 1.47 mmol g^{-1}, 0.200 g, 0.290 mmol) was washed with DCM (3 × 2 mL) and DMF (3 × 2 mL) and then swelled in dry DCM (2 mL) for 45 min. Bromoacetic acid (0.065 g, 0.470 mmol) and DIPEA (253 µL, 1.47 mmol) in dry DCM (2 mL) were added to the resin and the vessel was stirred on a shaker platform for 60 min at room temperature. After the resin was washed with DMF (3 × 2 mL), DCM (3 × 2 mL) and then with DMF (3 × 2 mL), a solution of proper amine (0,253 g, 2.90 mmol) in dry DMF (2 mL) was added to the bromoacetylated resin. The mixture was left on the shaker platform for 40 min at room temperature, and then the resin was washed with DMF (3 × 2 mL), DCM (3 × 2 mL) and then with DMF (3 × 2 mL). Subsequent bromoacetylation reaction was accomplished by reacting the oligomer with a solution of bromoacetic acid (0.400 g, 2.90 mmol) and DIC (494 µl, 3.20

mmol) in dry DMF (2 mL), stirring on a shaker platform for 40 min at room temperature. Then, the reaction with the amine was repeated as described above. The synthesis proceeded until the linear target was obtained. The oligomer-resin was cleaved by treatment with three aliquots of a solution of 20% HFIP in dry DCM (v/v; 3 × 2 mL), with stirring each time on the shaker platform for 30 min at room temperature and filtering the resin away after each treatment. The combined filtrates were concentrated in vacuo. The final product was analyzed by MALDI mass spectrometry and RP-HPLC (Figure S1-S5, ESI) and used for the cyclization step without further purification.

Linear precursor of 2a: white amorphous solid, 0.138 g, 36% yield; t_R: 9.3 min.; HRMS (MALDI): *m/z* $[M + H]^+$ Calcd for $C_{30}H_{57}N_6O_7^+$ 613.4283; Found 613.4252.

Linear precursor of 2d: white amorphous solid 0.279 g, 100% yield; t_R: 16.5 min.; HRMS (MALDI): *m/z* $[M + H]^+$ Calcd for $C_{54}H_{105}N_6O_7^+$: 949.8039; Found: 949.8074.

Linear precursor of 3a: white amorphous solid, 0.445 g, 100% yield; t_R: 14.0 min.; HRMS (MALDI): *m/z* $[M + H]^+$ Calcd for $C_{42}H_{57}N_6O_7^+$: 757.4283; Found: 757.4305.

Linear precursor of 3b : white amorphous solid, 0.354 g, 100% yield; t_R: 13.5 min.; HRMS (MALDI): *m/z* $[M + H]^+$ Calcd for $C_{45}H_{63}N_6O_7^+$: 799.4753; Found: 799.4699.

Linear precursor of 3c: white amorphous solid, 0.488 g, 100% yield; t_R: 15.8 min.; HRMS (MALDI): *m/z* $[M + H]^+$ Calcd for $C_{48}H_{69}N_6O_7^+$: 841.5222; Found 841.5279

General procedure for the high dilution cyclization: synthesis of 2a, 2d and 3a-c.

To a stirred solution of HATU (0.440 g, 1.16 mmol) and DIPEA (310 µl, 1.80 mmol) in dry DMF (80 mL) at room temperature, a solution of a linear precursor (0.29 mmol) in dry DMF (10 mL) was added using a syringe pump in 3 h. After 18 h the resulting mixture was concentrated in vacuo, diluted with DCM (100 mL) and washed with 1 M HCl (2 × 50 mL). The aqueous layer was extracted with DCM (2 × 100 mL) and the combined organic phases were washed with water (150 mL), dried over $MgSO_4$ and concentrated in vacuo. The crude cyclic peptoids were dissolved in hot ethyl acetate and precipitated by slowly cooling the solution.

2a: white amorphous solid, 0.068 g, 50% yield; t_R: 11.5 min; HRMS (MALDI): *m/z* $[M + Na]^+$ Calcd for $C_{30}H_{54}N_6NaO_6^+$: 617.3997; Found: 617.3986. ^{1}H NMR (400 MHz, $CDCl_3$, mixture of rotamers) δ: 4.75-2.88 (m, 24H, NC*H*$_2$CO and NC*H*$_2$CH$_2$CH$_3$ overlapped), 1.70-1.51 (m, 12H, NCH$_2$C*H*$_2$CH$_3$), 0.99-0.86 (m, 18H, NCH$_2$CH$_2$C*H*$_3$); ^{13}C NMR (150 MHz, $CDCl_3$) δ: 171.1, 170.1, 169.3, 167.5, 51.4, 51.3, 50.8, 50.6, 50,3, 49.8, 49.3, 48.8, 22.1, 22.0, 21.8, 21.7, 21.1, 21.0, 20.8, 20.6 11.3.

2d: white amorphous solid, 109 mg, 40% yield; Anal. Calcd for $C_{54}H_{102}N_6O_6$: C, 69.63; H, 11.04; N, 9.02. Found: C, 69.88; H, 11.01; N, 9.07; HRMS (ESI): *m/z* $[M + Na]^+$ Calcd for m/z $C_{54}H_{102}N_6NaO_6^+$: 953.7753; Found: 953.7698; ^{1}H NMR (400 MHz, $CDCl_3$, mixture of rotamers) δ: 5.22-2.62 (m, 12 H, COC*H*$_2$N and NC*H*$_2$(CH$_2$)$_5$CH$_3$ overlapped), 1.96-1.11 (m, 60 H, NCH$_2$(C*H*$_2$)$_5$CH$_3$), 0.88-0.84 (m, 18 H, N(CH$_2$)$_6$C*H*$_3$); ^{13}C NMR (100 MHz, $CDCl_3$) δ: 175.4, 171.3, 171.0, 169.8, 169.5, 169.2, 169.1, 168.8, 168.7, 168.3,168.2, 168.4, 168.0, 167.3, 166.5, 51.6, 51.1, 49.7, 49.4, 49.1, 48.9, 48.8, 48.6,48.5, 31.7, 28.9, 28.5, 27.7, 27.2, 26.8, 22.5, 14.0.

3a: white amorphous solid, 0.169 g, 39% yield; t_R: 12.9 min.; HRMS (ESI): *m/z* $[M + Na]^+$ Calcd for m/z $C_{42}H_{54}N_6NaO_6^+$: 761.3997; Found: 761.4030. ^{1}H NMR (600 MHz, $CDCl_3$, mixture of rotamers) δ: 7.59-7.02 (m, 15 H, Ar*H*), 4.91-2.94 (m, 24 H, NC*H*$_2$Ar, COC*H*$_2$N, NC*H*$_2$CH$_2$C*H*$_3$ overlapped), 1.82-1.25 (m, 6 H, NCH$_2$C*H*$_2$C*H*$_3$), 0.95-0.78 (m, 9 H, N(CH$_2$)$_2$C*H*$_3$); ^{13}C NMR (150 MHz, $CDCl_3$) δ: 171.9, 171.6, 171.0, 170.6, 170.1, 169.6, 169.2, 169.0, 168.7, 168.5, 168.4, 168.2, 167.9, 167.7, 167,3 166.6, 166.0, 137.5, 137.4, 137.0, 136.8, 136.5, 136.4, 135.8, 135.5, 135.2, 135.0, 129.3, 129.0, 128.9. 128.6, 128.5, 128.4, 128.3, 127.9, 127.7, 127.6, 127.5, 127.2, 127.1, 126.8, 126.5, 126.2, 126.1, 125.5, 125.3, 55.0, 54.4, 53.3, 52.7, 52.2, 52.1, 51.5, 51.4, 51.1, 51.0, 50.9, 50.7, 50.4, 50.3, 50.1, 50.0, 49.7, 49.6, 49.4, 49.2, 49.1, 49.0, 48.9, 48.7, 48.6, 48.4, 48.2, 47.9, 47.3, 47.1, 46.9, 46.8, 46.6, 46.3, 46.1, 44.3, 43.4, 22.7, 22.0, 21.8, 21.6, 21.3, 21.0, 20.8, 20.6, 20.1, 19.4, 18.4, 17.0, 11.1, 11.0, 10.9, 10.7.

3b: white amorphous solid, 0.118, 34% yield; t_R: 15.6 min. ; HRMS (ESI): *m/z* $[M + Na]^+$ Calcd for m/z $C_{45}H_{60}N_6NaO_6^+$: 803.4467; 803.4498.^{1}H NMR (600 MHz, $CDCl_3$, mixture of rotamers) δ: 7.57-7.01 (m, 15 H, Ar*H*), 5.58-2.97 (m, 24 H, NC*H*$_2$Ar, COC*H*$_2$N, NC*H*$_2$(C*H*$_2$)$_2$CH$_3$ overlapped), 1.71-1.12 (m, 12 H, NCH$_2$(C*H*$_2$)$_2$CH$_3$), 0.97-0.71 (m, 9 H, N(CH$_2$)$_2$C*H*$_3$); ^{13}C NMR (150 MHz, $CDCl_3$) δ: 171.8, 171.2, 171.1, 170.2, 169.6, 169.5, 169.3, 169.1, 168.6, 168.5, 168.1, 167.8, 167.3, 166.6, 136.9, 136.8, 136.6, 135.9, 135.7, 135.3, 129.3, 129.2, 129.0, 128.9, 128.8, 128.6, 128.5, 128.3, 128.2, 128.1, 128.0, 127.9, 127.8, 127.7, 127.4, 127.2, 126.9, 126.8, 126.8, 126.7, 126.3, 125.7, 125.6, 125.4, 52.9, 51.6, 51.5, 51.0, 50.1, 49.8, 49.5, 49.0, 48.9, 48.8, 48.7, 48.3, 48.2, 47.9, 47.4, 30.8, 30.6, 30.0, 29.9, 29.7, 29.5, 29.4, 29.1, 20.0, 20.0, 19.8, 13.9, 13.8, 13.7, 13.6.

3c: white amorphous solid, 0.234, 49% yield; Anal. Calcd for $C_{48}H_{66}N_6O_6$: C, 70.04; H, 8.08; N, 10.21. Found: C, 70.17; H, 8.11; N, 10.15; HRMS (ESI): *m/z* $[M + Na]^+$ Calcd for m/z $C_{48}H_{66}N_6NaO_6^+$: 845.4936; Found: 845.5039. ^{1}H NMR (600 MHz, $CDCl_3$, mixture of rotamers) δ: 7.57-7.04 (m, 15 H, Ar*H*), 5.77-2.78 (m, 24 H, NC*H*$_2$Ar, COC*H*$_2$N, NC*H*$_2$(C*H*$_2$)$_2$CH$_3$ overlapped), 1.72-1.09 (m, 18 H, NCH$_2$(C*H*$_2$)$_3$CH$_3$), 0.95-0.80 (m, 9 H, N(CH$_2$)$_2$C*H*$_3$); ^{13}C NMR (150 MHz, $CDCl_3$) δ: 171.8, 171.0, 170.1, 169.6, 169.4, 169.0, 168.6, 168.5, 168.2, 167.7, 167.3, 166.6, 166.0, 136.9, 136.8, 136.6, 136.0, 135.3, 129.1, 128.9, 128.7, 128.6, 128.5, 128.3, 128.2, 128.1, 128.0, 127.9, 127.8, 127.6, 127.3, 127.1, 126.9, 126.8, 125.7, 125.6, 125.4, 54.6, 53.2, 53.1, 52.9, 52.2, 51.6, 51.5, 51.2, 51.0, 50.8, 50.4, 50.1, 50.0, 49.8, 49.5, 49.3, 49.0, 48.9, 48.8, 48.7, 48.3, 48.2, 48.0, 47.4, 47.2, 46.8, 46.7, 46.5, 46.2, 45.7, 43.5, 31.9, 30.8, 30.6, 30.4, 30.0, 29.9, 29.7, 29.5, 29.3, 28.4, 20.3, 20.1, 20.0, 19.9, 13.9, 13.8, 13.7, 13.6, 13.4.

Procedure for the formation of the Na^+ complex of 3a

To a 10.0 mM solution of **3a** (2.7 mg, 0.005 mmol) in $CDCl_3$ (0.5 mL) were added increasing amounts of NaTFPB until 1.0 equiv. After every addition, the mixture was sonicated for 5 min, and the NMR spectrum was recorded.

3a·[Na^+TFPB$^-$]: ^{1}H NMR (400 MHz, $CDCl_3$) δ: 7.70 (s, 8H, TFPB-o-H), 7.51 (s, 4H, TFPB-p-H), 7.37-7.36 (m, 8H, ArH), 7.23-7.21 (m, 7H, ArH), 4.88 (d, 2H, *J* = 16.4 Hz, NC*H*$_2$Ar), 4.81-4.71 (m, 4H, COC*H*$_2$N), 4.37 (d, 2H, *J* = 16.4 Hz, NC*H*$_2$Ar), 3.57-3.48 (m, 6H, COC*H*$_2$N, NC*H*$_2$Ar), 3.18-3.15 (t, 6H, *J* = 7.3 Hz, NC*H*$_2$CH$_2$CH$_3$), 1.59-1.48 (m, 10H, COC*H*$_2$N, NCH$_2$C*H*$_2$CH$_3$), 0.84 (t, 9H, *J* = 7.3 Hz, NCH$_2$CH$_2$C*H*$_3$).

Crystallization

5 mg of compound **2a** were dissolved in 1.0 mL of hot ethyl acetate. Colourless platelets suitable for X-ray diffraction analysis were obtained after a few days.

Single crystal X-ray diffraction

A single crystal of **2a** was selected and mounted on a MiTeGen microloop with paratone oil. X-ray diffraction data were collected at 296 K with a Bruker D8 QUEST diffractometer equipped with a PHOTON II detector using Cu*K*α radiation (λ= 1.54178 Å). Data indexing was performed using APEX3.[21] Data integration and reduction were performed using SAINT.[21] Absorption correction was performed by a multi-scan method in SADABS.[22]

Crystal structure determination

The crystal structures were solved by direct methods using SHELXS-97[23] and refined by means of full matrix least-squares based on F^2 using the program SHELXL.[24] Non-hydrogen atoms were refined anisotropically, hydrogen atoms were positioned geometrically and included in structure factors calculations but not refined. *OLEX2* was used as GUI.[25]

Type I molecule shows positional disorder on the *cis* propyl side chains attached to the nitrogen atom N1A. In particular, the last carbon atom can occupy two different positions with refined occupancy of 0.660(7) and 0.340(7). Restraints on anisotropic displacement parameters of disordered atoms were used.

Relevant crystallographic data and structure refinement details are listed in Table S1 (ESI), ORTEP are shown in Figure S21 (ESI).

Ion transport studies

General procedures. Egg yolk phosphatidylcholine (EYPC, 100 mg/mL chloroform solution), cholesterol and 8-hydroxypyrene-1,3,6-trisulfonic acid trisodium salt (HPTS) were from Sigma; Triton® X-100 and HEPES buffer were from Fluka; all salts were of the best grade available from Aldrich and were used without further purification. Liposomes were prepared by extrusion using a 10 mL LipexTM Thermobarrel EXTRUDER (Northern Lipids Inc.) connected to a thermostatic bath maintained at 25 °C. 100 nm polycarbonate membranes were Nucleopore Track-Etch Membranes from Whatman. Fluorescence spectra were recorded on a Varian Cary Eclipse fluorescence spectrophotometer. All fluorimetric measurements were performed at 25 °C. The ionophore concentration is given in percent with respect to the total concentration of lipids. Mother solutions of compounds **2** and **3** were prepared in MeOH and DMSO, respectively. Control experiments showed that the amount of MeOH and DMSO added to the vesicular suspension in the different experiments (maximum amount: 8% in volume) did not affect the permeability of the membrane. The logP values of compounds **2** and **3** were calculated using the ALOGPs 2.1 software (VCCLAB, V.C.C.L., http://www.vcclab.org).

HPTS assay. 150 µL of EYPC chloroform solution (100 mg/mL, 20 µmol) was first evaporated under Ar-flux to form a thin film and then dried under high vacuum for 3 h. If required, 66 µL of cholesterol chloroform solution (50 mg/mL, 8.5 µmol) or the desired amount of cyclopeptoid dissolved in chloroform were added. The lipid cake was hydrated in 1.5 mL of 0.1 mM HPTS solution (25 mM HEPES, 100 mM NaCl, pH 7) for 30 min at 40 °C. The lipid suspension was subjected to five freeze–thaw cycles (−196 °C/40 °C) using liquid nitrogen and a thermostatic bath, and then extruded under nitrogen pressure (15 bar) at room temperature (10 extrusions through a 0.1 µm polycarbonate membrane). The LUV suspension was separated from the extravesicular dye by size exclusion chromatography (SEC) (stationary phase: pre-packed column Sephadex™ G-25, mobile phase: 25 mM HEPES buffer, 100 mM NaCl, pH 7) and diluted with HEPES buffer (25 mM HEPES, 100 mM NaCl, pH 7) to give a stock solution with a lipid concentration of 5 mM (assuming 100% of lipids were incorporated into liposomes). 104 µL of the lipid suspension were placed in a fluorimetric cell and diluted to 3040 µL with the appropriate buffer solution (25 mM HEPES, pH 7) containing 100 mM of the salt under investigation (MCl with M = Li^+, Na^+, K^+, Rb^+, Cs^+; NaX with X = Cl^-, Br^-, I^-). The total lipid concentration in the fluorimetric cell was 0.17 mM. An aliquot of the solution of the ionophore in MeOH or DMSO (10–80 µL of the appropriate mother solution in order to obtain the desired $mol_{compound}/mol_{lipid}$ ratio) was then added to the lipid suspension and the cell was incubated at 25 °C for 10 min. After incubation, the time course of fluorescence was recorded for 50 s monitoring the HPTS emission at 510 nm with excitation wavelengths set alternately at 403 and 460 nm on a 0.5 + 0.5 s cycle. Then 50 µL of 0.5 M MOH (with M = Li^+, Na^+, K^+, Rb^+, Cs^+; depending on the cation present in the extravesicular solution) were rapidly added through an injector port and the fluorescence emission was recorded for 800 s. In the case of the experiment with the protonophore, a DMSO solution of CCCP (10 µL, 0.52 mM), in order to get a concentration of 1%, was added at 50s and the solution of MOH was added at 100 s. In each experiment, maximal changes in dye emission were obtained by the final lysis of the liposomes with a detergent (40 µL of 5% aqueous Triton® X-100). The data set consists of emission intensities at 510 nm modulated by alternating excitation at 403 nm and 460 nm on a 0.5 + 0.5 s cycle. The concentration of the conjugate base form of HPTS is related to the emission intensity at 510 nm during the period in which the dye is excited at 460 nm (E460) while the concentration of the protonated form is

$$FI = \frac{\left(\frac{E_{403}}{E_{460}}\right)_t - \left(\frac{E_{403}}{E_{460}}\right)_0}{\left(\frac{E_{403}}{E_{460}}\right)_\infty - \left(\frac{E_{403}}{E_{460}}\right)_0} \times 100$$

related to the emission intensity at 510 nm during the period in which the dye is excited at 403 nm (E403). Fluorescence time courses were normalized using the following equation, where the subscripts 0, ∞ and t denote the emission ratios before the base pulse, after detergent lysis, and at an intermediate time, respectively.

Acknowledgements

Financial support from the University of Salerno (FARB). We thank Dr. Assunta D'Amato and Miss Alicja Malgorzata Araszczuk, University of Salerno, for experimental work; Dr. Patrizia Iannece, University of Salerno, for HR-MS and Dr. Patrizia Oliva, University of Salerno, for NMR spectra. M. Tosolini, J. ur Rehman, M. Raza Shah, and P. Tecilla thank the EU for the MC-RISE INFUSION research project (grant N. 734834).

Keywords: cyclic peptoids• peptidomimetics • macrocycles • ionophores • ion carriers

[1] S. K. J. Berezin, *Membr. Biol.* **2015**, *248*, 713−726.

[2] M. Kamyar, P. Rawnduzi, C. R. Studenik, K. Kouri, R. Lemmens-Gruber, *Arch. Biochem. Biophys.* **2004**, *429*, 215−223.

[3] C. De Cola, S. Licen, D. Comegna, E. Cafaro, G. Bifulco, I. Izzo, P. Tecilla, F. De Riccardis, *Org. Biomol. Chem.* **2009**, 7, 2851−2854.

[4] L. A. Jowett, E. N. W. Howe, X. Wu, N. Busschaert, P. A. Gale, *Chem. Eur. J.* **2018**, *24*, 10475−10487.

[5] See for example: a) A. V. Koulov, T. N. Lambert, R. Shukla, M. Jain, J. M. Boon, B. D. Smith, H. Li, D. N. Sheppard, J.-B. Joos, J. P. Clare, A.

P. Davis, *Angew. Chem. Int. Ed*. **2003**, *42*, 4931–4933; b) J. A. Cooper, S. T. G. Street, A. P. Davis, *Angew. Chem. Int. Ed*. **2014**, *53*, 5609–5613; c) H. Valkenier, L. W. Judd, H. Li, S. Hussain, D. N. Sheppard, A. P. Davis, *J. Am. Chem. Soc.* **2014**, *136*, 12507–12512 d) S. J. Moore, C. J. E. Haynes, J. González, J. L. Sutton, S. J. Brooks, M. E. Light, J. Herniman, G. J. Langley, V. Soto-Cerrato, R. Pérez-Tomás, I. Marques, P. J. Costa, V. Félix, P. A. Gale, *Chem. Sci.* **2013**, *4*, 103–117; e) N. Busschaert, I. L. Kirby, S. Young, S. J. Coles, P. N. Horton, M. E. Light, P. A. Gale, *Angew. Chem.: Int. Ed*. **2012**, 51, 4426–4430; f) L. W. Judd A. P. Davis, *Chem. Comm.* **2010**, *46*, 2227–2229; g) B. A. McNally, A. V. Koulov, T. N. Lambert, B. D. Smith, J.-B. Joos, A. L. Sisson, J. P. Clare, V. Sgarlata, L. W. Judd, G. Magro A. P. Davis, *Chem. Eur. J.* **2008**, *14*, 9599–9606.

[6] a) H. C. Visser, D. N. Reinhoudt, F. de Jong, *Chem. Soc. Rev.* **1994**, 23, 74–81; b) A. P. Davis, D. N. Sheppard, B. D. Smith, *Chem. Soc. Rev.* **2007**, *36*, 348–357.

[7] a) N. J. Knight, E. Hernando, C. J. E. Haynes, N. Busschaert, H. J. Clarke, K. Takimoto, M. García-Valverde, J. G. Frey, R. Quesada, P. A. Gale, *Chem. Sci.* **2016**, *7*, 1600−1608; b) N. Busschaert, S. J. Bradberry, M. Wenzel, C. J. E. Haynes, J. R. Hiscock, I. L. Kirby, L. E. Karagiannidis, S. J. Moore, N. J. Wells, J. Herniman, G. J. Langley, P. N. Horton, M. E. Light, I. Marques, P. J. Costa, V. Felix, J. G. Frey, P. A. Gale, *Chem. Sci.* **2013**, *4*, 3036−3045; c) S. J. Edwards, I. Marques, C. M. Dias, R. A. Tromans, N. R. Lees, V. Félix, H. Valkenier, A. P Davis, *Chem. Eur. J.* **2016**, *22*, 2004−2011; d) C. J. E. Haynes, N. Busschaert, I. L. Kirby, J. Herniman, M. E. Light, N. J. Wells, I. Marques, V. Felix, P. A. Gale, *Org. Biomol. Chem*. **2014**, *12*, 62−72; e) V. Saggiomo, S. Otto, I. Marques, V. Félix, T. Torroba, R. Quesada, *Chem. Comm.* **2012**, *48*, 5274−5276; f) M. J. Spooner, P. A. Gale, *Chem. Comm.* **2015**, *51*, 4883−4886; g) H. Valkenier, C. J. E. Haynes, J. Herniman, P. A. Gale, P. A. Davis, *Chem. Sci.* **2014**, *5*, 1128−1134.

[8] C. M. Dias, H. Li, H. Valkenier, L. E. Karagiannidis, P. A. Gale, D. N. Sheppard, A. P. Davis, *Org. Biomol. Chem.* **2018**, *16*, 1083−1087.

[9] L. Zhi, C. Wen-Hua, *Mini-Rev. Med. Chem.* **2017**, *17*, 1398−1405.

[10] W. M. Leevy, M. E. Weber, M. R. Gokel, G. B. Hughes-Strange, D. D. Daranciang, R. Ferdani, G. W. Gokel, *Org. Biomol. Chem.* **2005**, *3*, 1647−1652.

[11] A. Meli, S. Gambaro, C. Costabile, C. Talotta, G. Della Sala, P. Tecilla, D. Milano, M. Tosolini, I. Izzo, F. De Riccardis, *Org. Biomol. Chem.*, **2016**, *14*, 9055−9062.

[12] A. D'Amato, R. Volpe, M. C. Vaccaro, S. Terracciano, I. Bruno, M. Tosolini, C. Tedesco, G. Pierri, P. Tecilla, C. Costabile, G. Della Sala, I. Izzo, F. De Riccardis, *J. Org. Chem.* **2017**, *82*, 8848−8863.

[13] R. Schettini, C. Costabile, G. Della Sala, J. Buirey, M. Tosolini, P. Tecilla, M. Vaccaro, I. Bruno, F. De Riccardis, I. Izzo, *Org. Biomol. Chem.* **2018**, *16*, 6708–6717.

[14] **2b** and **2c** were prepared as previously described. **2b**: a) G. Della Sala, B. Nardone, F. De Riccardis, I. Izzo, *Org. Biomol. Chem.*, **2013**, *11*, 726–734; **2c**: b) G Pierri, R. Schettini, J. Nuss, R. E. Dinnebier, F. De Riccardis, I. Izzo, C. Tedesco *Cryst. Eng. Comm.*, **2020**, accepted manuscript, DOI: 10.1039/D0CE01136C.

[15] R. N. Zuckermann, J. M. Kerr, S. B. H. Kent, W. H. Moos, *J. Am. Chem. Soc.*, **1992**, *114*, 10646−10647.

[16] C. De Cola, G. Fiorillo, A. Meli, S. Aime, E. Gianolio, I. Izzo and F. De Riccardis, *Org. Biomol. Chem*. **2014**, *12*, 424−431.

[17] A. D'Amato, R. Schettini, G. Della Sala, C. Costabile, C. Tedesco I. Izzo, F. De Riccardis, *Org. Biomol. Chem*. **2017**, *15*, 9932−9942.

[18] N. R. Clement, J. M. Gould, *Biochem.* **1981**, *20*, 1534–1538.

[19] N. Sakai, S. Matile, *J. Phys. Org. Chem.*, **2006**, *19*, 452–460.

[20] N. Busschaert, L. E. Karagiannidis, M. Wenzel, C. J. E. Haynes, N. J. Wells, P. G. Young, D. Makuc, J. Plavec, K. A. Jolliffe, P. A. Gale, *Chem. Sci.* **2014**, *5*, 1118.

[21] Bruker Suite, Version 2013/1. Bruker AXS Inc., Madison, WI, USA, 2013.

[22] G. M. Sheldrick, Bruker (**2014**) SADABS, version 2014/5, Bruker AXS Inc., Madison, Wisconsin, USA.

[23] G. M. Sheldrick, *Acta Cryst. A,* **2008**, *64*, 112–122.

[24] G. M. Sheldrick, *Acta Cryst. C*, **2015**, *71*, 3–8.

[25] O. V. Dolomanov, L. J. Bourhis, R. J. Gildea, J. A. K Howard, H. J. Puschmann, *Appl. Cryst.*, **2009**, *42*, 339–341.

…

Entry for the Table of Contents

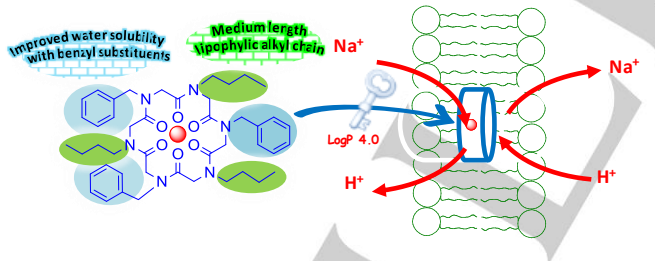

The crucial role of lipophilicity on ionophoric properties of hexameric cyclic peptoids is discussed. A fine tuning of *N*-alkyl side chains was realized in order to improve the activity of these versatile class of ionic carriers.